AEOLIAN LANDFORMS IN THE EXOMARS 2028 LANDING SITE. S. Silvestro[1,2], D.A. Vaz[3,1], F.M. Grasso[4], L.K. Fenton[2], R. Cardoso[3], A. Pacifici[5], D. Tirsch[6], E. Favaro[7], Y. Tao[8], F. Salese[5], C.I. Popa[1], G. Franzese[1], G. Mongelluzzo[1], C. Porto[1], M. Pajola[9], F. Esposito[1]. [1]INAF, Osservatorio Astronomico di Capodimonte, Napoli, Italy (simone.silvestro@inaf.it). [2]SETI Institute, Mountain View, CA, USA. [3]CITEUC, University of Coimbra, Portugal. [4]CNR ISAC Lecce, Italy. [5]IRSPS, Università G. d'Annunzio, Chieti-Pescara, Italy, [6]Inst. Planetary Res., DLR, Berlin, Germany. [7]ESA/ESTEC, Noordwijk, the Netherlands. [8]Freie University, Berlin, Germany. [9]INAF, Osservatorio Astronomico di Padova, Italy.

Intro & methods: The ESA ExoMars mission will land at Oxia Planum to search for signs of life on Mars [1, 2] (Fig. 1a). Dust devil tracks, bright bedforms (transverse aeolian ridges [TARs]), and erosive wind-formed ridges (periodic bedrock ridges [PBRs]) have been documented in the landing site [3-6]. In this study, we compare automated and manual mapping of aeolian features in CTX (6 m/pixel), CaSSIS (5 m/pixel) and HiRISE (25 cm/pixel) images in the landing site (Fig. 1) with potential sand fluxes from the NASA Ames GCM [7]. In particular, we focus our attention on bright bedforms, ridges and wind streaks (Fig. 1). Because these features are widespread on Mars, observations made here on PBRs and TARs are also relevant for other areas, such as those explored by Opportunity [8, 9], Curiosity [10], Perseverance [11], and Zhurong [12, 13].

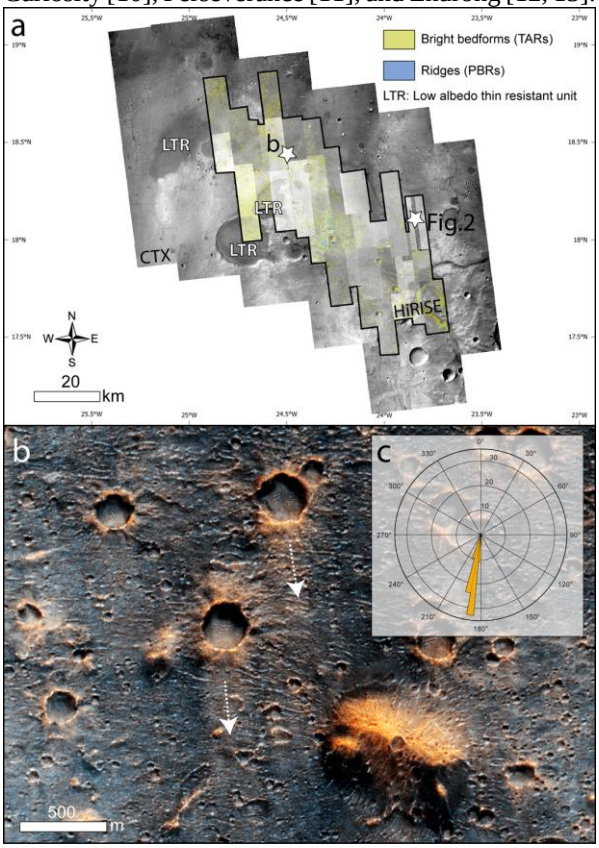

Fig. 1: (a) Automatically mapped PBRs and TARs within the study area (CTX and HiRISE mosaics [14]). **(b, c)** Wind streak orientations in the landing area (CaSSIS RGB image MY35_007623_019_0).

Results: Different aeolian features can be seen in the landing area.

Wind streaks (n = 87) were manually mapped on the CTX image mosaic in a GIS environment. Most of the mapped streaks are bright-toned (n = 85), indicating winds originating from the NNW–NNE (Fig. 1b, c). A few dark-toned streaks (n = 2), formed by winds from the E–ESE, were also identified. Similar wind streak orientations observed outside the landing ellipse suggest a regional origin for these flows.

Bright bedforms (TARs) were automatically mapped within the study area using the method described in [15]. They are widespread and exhibit dark banding on their SE-facing slopes [4]. Notably, similar albedo variations on bright-toned dune-like features or TARs have been reported at the Tianwen-1 Zhurong and NASA Perseverance landing sites [11-13].

Ridges (PBRs) were automatically mapped as well (Fig. 1a). Together with the bright-toned ridge set carved in the clay-enriched Noachian bedrock [4-6], here, we identified a potentially new class of WNW–ESE-oriented cratered ridges ("ridges 2" in Fig. 2). These features, located inside degraded impact craters, display Y-junctions and may be locally covered by boulders from nearby impacts [4] (Fig. 2). However, unlike PBRs, they are not directly carved into the underlying bedrock (Fig. 2). Interestingly, this ridge set is also observed within craters on the low albedo thin resistant (LTR) unit [4], which is widespread in Oxia Planum [14, 16] (Fig. 1).

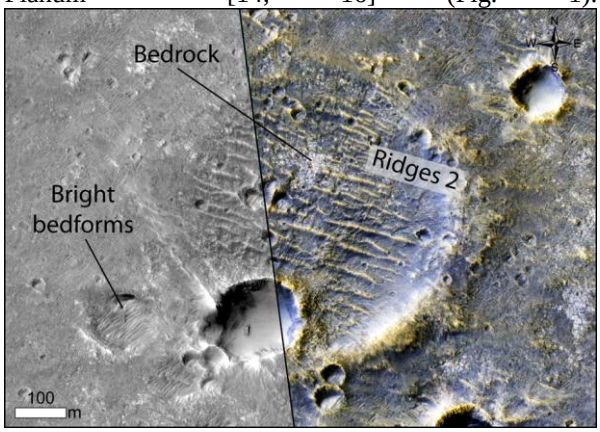

Fig. 2: WNW-ESE ridges inside an eroded impact crater (HiRISE ESP_062481_1985). The ridges directly overlay the bright, clay-bearing Noachian bedrock [2].

Discussion: The consistent orientation of bright wind streaks in the study area suggests contemporary regional winds predominantly blowing from the north, corresponding to the return flows of the Hadley cell circulation [17]. We also identified a secondary mode formed by winds from the ESE. Interestingly, a bimodal sand flux direction is also predicted by the GCM (Fig. 3), with one mode (~172°–188°) closely matching the observed bright-toned wind streak orientations (Fig. 1b, c). This, along with no observed changes in orientation or modification of the bright streaks, indicates that these winds continue to blow at the surface and/or that winds from other directions are not strong or frequent enough to rework the wind streaks.

Bright bedforms (TARs) are likely relict features shaped by past wind conditions [4, 5]. This is supported by the GCM-predicted bedform orientation (red line in Fig. 3), which does not align with either the observed TARs' orientation or that of the older periodic bedrock ridges (PBRs) [4-6]. Identified albedo variations on TARs' SW slopes might be caused by aeolian sorting of loose sands with varying granulometry and/or composition. This suggests formative winds distinct from those previously inferred [4]. Alternatively, these variations might reflect transitions between crusted and non-crusted surfaces, similar to those observed at the Zhurong landing site [12].

The newly identified "ridge 2" class of landform has previously been interpreted as precursor bedforms that initiated the formation of the underlying PBRs [4]. This interpretation is supported by (1) the close spatial association between PBRs and the "ridge 2" class, and (2) their similar orientation. However, in the example shown in Fig. 2, the ridges are located on a flat bedrock surface and are not associated with PBRs. This observation raises the possibility that these features may represent a later episode of aeolian deposition or erosion, occurring after the formation of the PBRs [4]. This hypothesis is consistent with the presence of the "ridge 2" class inside craters over the LTR unit (indicating post-dating of the unit emplacement) and recent age estimates for the PBRs [6]. The morphology of the "ridge 2" class varies across the study area, with some ridges appearing subdued and eroded. A ghost-dune pit origin [18] and/or an erosional-scarf/bedform assemblage, similar to observations at Meridiani Planum (see Fig. 6b in [9]), cannot be ruled out.

Detailed examination of the relationships among ridges, PBRs, and TARs by the ESA Rosalind Franklin rover will be crucial for advancing our understanding of PBR formation mechanisms, the winds responsible for shaping TARs, and broader Martian climatic changes [8, 9, 19, 20].

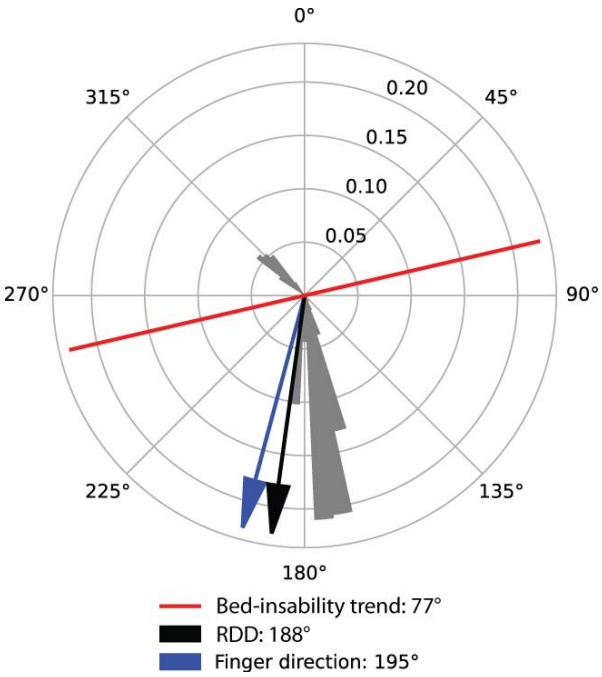

Fig. 3: GCM output at 18.2°N, 24.3°W. RDD represents the resultant drift direction [21]. The red line indicates the predicted orientation assuming the bed-instability mode as the bedform formation model [22, 23]. "Finger direction" refers to the bedform elongation direction, assuming the fingering mode as the formation mechanism [23].

References: [1] Vago J. et al. (2017). Astrobiology, 17. [2] Quantin et al. (2021), Astrobiology, 21. [3] Balme M. et al. (2017), PSS, 153, 39-53. [4] Silvestro S. et al. (2021), GRL, 48. [5] Favaro E. et al. (2021), JGR, 126. [6] Favaro E. et al. (2024), EPSL, 626. [7] Haberle R.M. et al. (2003), Icarus, 161. [8] Golombek M. et al. (2010), JGR, 115, 1-34. [9] Fenton L.K. et al. (2018), JGR, 123, 1–15. [10] Stack K.M. et al. (2022), JGR, 127, e2021JE007096. [11] Sullivan et al. (2022), 53rd LPSC, 2887. [12] Lu Y. et al. 2022, EPSL, 595, 117785. [13] Gou S. et al. 2022, EPSL, 595, 117764. [14] Fawdon et al. (2024), Journal of Maps, 20(1), 2302361. [15] Vaz D.A. et al. (2023), EPSL, 614. [16] Harris E. et al. (2024), JGR, 129. [17] Greeley et al. (1993), JGR, 98, E2, 3183-3196. [18] Day M.D. & Catling D.C. (2018), JGR, 123. [19] Montgomery D.R. et al. (2012), JGR, 117, E03005. [20] Hugenholtz C.H. et al. (2015), Aeol. Res., 18, 135–144. [21] Fryberger S.G. & Dean G. (1979), USGS prof.paper, 1052. [22] Rubin D.M. & Hunter R.E. (1987), Science, 237. [23] du Pont S.C. et al. (2014), Geology, 42. **Acknowledgement:** The results reported here were obtained in the context of the Earth-Moon-Mars (EMM) project, led by INAF in partnership with ASI & CNR, funded under the National Recovery and Resilience Plan, Mission 4, Component 2, Investment 3.1: "Fund for the realisation of an integrated system of research and innovation infrastructures" Action 3.1.1 funded by the EU, NextGenerationEU.